Available online at www.sciencedirect.com
ScienceDirect
Applied Catalysis A: General 316 (2007) 175–183
APPLIED CATALYSIS A: GENERAL
www.elsevier.com/locate/apcata

Study of Ni and Pt catalysts supported on α-Al_2O_3 and ZrO_2 applied in methane reforming with CO_2

Francisco Pompeo [a,b], Nora N. Nichio [a,b], Mariana M.V.M. Souza [c,d], Deborah V. Cesar [c], Osmar A. Ferretti [a,b,*], Martin Schmal [c,d,*]

[a] CINDECA, Facultad de Ciencias Exactas, UNLP-CONICET, 47 No. 257, 1900 La Plata, Argentina
[b] Facultad de Ingeniería, Universidad Nacional de La Plata, 1 Esq 47, 1900 La Plata, Argentina
[c] NUCAT/PEQ/COPPE, Universidade Federal do Rio de Janeiro, C.P. 68502, 21945-970 Rio de Janeiro, Brazil
[d] Escola de Química, Universidade Federal do Rio de Janeiro, C.P. 68542, 21940-900 Rio de Janeiro, Brazil

Received 5 May 2006; received in revised form 30 August 2006; accepted 4 September 2006
Available online 4 October 2006

Abstract

Ni and Pt catalysts supported on α-Al_2O_3, α-Al_2O_3-ZrO_2 and ZrO_2 were studied in the dry reforming of methane to produce synthesis gas. All catalytic systems presented well activity levels with TOF (s^{-1}) values between 1 and 3, being Ni based catalysts more active than Pt based catalysts. The selectivity measured at 650 °C, expressed by the molar ratio H_2/CO reached values near to 1. Concerning stability, Pt/ZrO_2, Pt/α-Al_2O_3-ZrO_2 and Ni/α-Al_2O_3-ZrO_2 systems clearly show lower deactivation levels than Ni/ZrO_2 and Ni or Pt catalysts supported on α-Al_2O_3. The lowest deactivation levels observed in Ni and Pt supported on α-Al_2O_3-ZrO_2, compared with Ni and Pt supported on α-Al_2O_3 can be explained by an inhibition of reactions leading to carbon deposition in systems having ZrO_2. These results suggest that ZrO_2 promotes the gasification of adsorbed intermediates, which are precursors of carbon formation and responsible for the main deactivation mechanism in dry reforming reaction.

Keywords: Methane; Carbon dioxide; Syngas; Reforming; Nickel; Platinum

1. Introduction

Methane reforming reactions have been employed to produce hydrogen or synthesis gas. Due to the increase of H_2 demand and the importance of synthesis gas as a major feedstock for fuel cells and Fischer–Tropsch reaction, methane reforming catalysts have become more and more important.

Most VIII group metals, especially noble metal and Ni based catalysts, have been studied for steam reforming, dry reforming, partial oxidation and mixed reforming of methane [1–5]. The catalyst deactivation is the main hindrance for a catalyst to be considered for an industrial application, the two most known causes are: coke deposition and sintering of the metallic active phase. Most of the authors agree that coke formation is the main cause of deactivation. Carbon deposition results from two reactions, Boudouard reaction ($2CO \rightarrow C + CO_2$) and/or methane decomposition ($CH_4 \rightarrow C + 2H_2$). The type and the nature of coke formed depend on the metal and in many cases on the support used.

Ni catalysts seem to be the most interesting ones due to its lower cost; their main disadvantage is the high rate of carbon formation. For Ni catalysts, the metal can dissolve unreactive C residues and generate carbon filaments (whiskers) with the Ni particle on the filament top [1,6]. During this process, metallic sites remain uncovered despite the deposition of large amounts of carbon, thus resulting in much lower deactivation rates than those expected if metal covering coke deposits occurred [7–10]. However, whisker formation must absolutely be avoided because it causes a significant expansion of the catalyst bed resulting in severe operational problems. Besides, as Ni is placed on the filament top, it is difficult to regenerate the catalytic system because the contact between metal and support is lost.

Several studies have been performed in order to improve the coke resistance of Ni based catalysts. The formation of $NiAl_2O_4$

* Corresponding authors. Tel.: +54 221 4254277; fax: +54 221 4220288.
E-mail addresses: fpompeo@quimica.unlp.edu.ar (F. Pompeo), ferretti@quimica.unlp.edu.ar (O.A. Ferretti), schmal@peq.coppe.ufrj.br (M. Schmal).

0926-860X/$ – see front matter © 2006 Elsevier B.V. All rights reserved.
doi:10.1016/j.apcata.2006.09.007

during pretreatments results in a sharp decrease in carbon content and also similar results have been reported when working with "solid solutions" of NiO–MgO, being this fact related to the size of the formed crystals [11–13].

The addition of metallic promoters, such as Sn, leads to catalysts with a very high resistance to carbon deposition and this may be explained by considering that carbon formation reactions are more structure sensitive than syngas formation reactions [14]. The carbon deposition also decreases when Ni is deposited on supports that present a marked Lewis basicity or on supports that have been modified for that purpose with alkaline metals such as Li or K [15–17].

Noble metals are known to form less coke under reforming reactions and the coke formed differs in nature from that found with Ni catalysts. On noble metals (Ru, Rh, Pt and Ir), coke is thought to block the metal and to induce deactivation because of the loss of surface metal atoms. There exist debates and controversies among authors about which of these metals present the best performances [18–21]. Although the Rh seems to be the one that better fulfills with the compromise between activity and stability, platinum is an interesting metal to be used as catalyst for syngas obtention due to good availability and its relatively low price with respect to rhodium. For Pt/Al_2O_3 catalysts, Nagaoka et al. reported that Pt particles are gradually covered by a coke monolayer, which is correlated to an initial deactivation in dry reforming [22]. In the same paper authors observed that the rate of CH_4 decomposition on Pt/ZrO_2 is slower than that on Pt/Al_2O_3, and this is explained as a result of a better balance between carbon formation and its oxidation by the activated CO_2 at the perimeter of the metal–support interface on Pt/ZrO_2 sample. In another paper, the same authors concluded that coke is more reactive towards CO_2 in the case of Pt/ZrO_2 [23]. Jung et al., by using periodic DFT calculations for Pt/ZrO_2, reported the evidence of electronic modifications in platinum atom indicating an electron transferred from the metal to the ZrO_2 giving place to a strong interaction between metal and support [24].

Supports such as CeO_2 and/or ZrO_2 present properties that make them interesting for their use as modifiers of reforming catalysts. These properties may be the improvement of metallic dispersion, the sintering decrease, the improvement of thermal stability and the enhancement of oxygen storage capacity [25,26], helping, in this way, the gasification of carbon formed during the reforming.

In the present contribution, we consider the advantages of ZrO_2 for its use as modifier of commercially available α-Al_2O_3 support before impregnating Ni and Pt. Although the γ-Al_2O_3 is one of the most used supports in references, it is thermally unstable at high temperatures (>600 °C) since γ-Al_2O_3 suffers a transformation process into the more thermally stable α-Al_2O_3 phase. α-Al_2O_3 presents, besides its stability, high mechanical resistance and for this reason it is an adequate support for the industrial process.

The performance of Ni and Pt catalysts supported on α-Al_2O_3, α-Al_2O_3 modified by ZrO_2 and pure ZrO_2 is evaluated in the methane reforming reaction with CO_2; this reaction is chosen for the stability study of these catalytic systems, since it is highly sensitive to deactivation by carbon deposition, as it has been previously reported [14].

2. Experimental

2.1. Catalyst preparation

Catalysts were prepared by using three supports α-Al_2O_3 (A), α-Al_2O_3 modified by ZrO_2 (AZ) and ZrO_2 (Z). The α-Al_2O_3 support was obtained by Rhone Poulenc. The support α-Al_2O_3-ZrO_2 (ZrO_2 content 1 wt%) was the same alumina modified by impregnation with a solution of zirconium hydroxide in HNO_3 (50%, v/v) and subsequent calcination in air (16 h at 550 °C). The ZrO_2 support was obtained by calcination of $Zr(OH)_4$ (Mels Chemicals) at 550 °C for 2 h at air flow [27].

Catalysts were prepared by impregnation of supports previously calcined by an aqueous solution of nickel nitrate and an aqueous solution of hexachloroplatinic acid, with proper concentrations for obtaining a final loading of 2 wt% in Ni and 1 wt% in Pt.

2.2. Catalyst characterization

The surface area and the distribution of the support pore size were measured by nitrogen adsorption at 77 K by using commercial equipment Accusorb 2100E Micromeritics. The samples were degasified at 100 °C for 12 h before adsorption.

Transmission electron microscopy (TEM) images were taken by means of a TEM JEOL FX 2000. A graphite pattern was used for calibration. In this analysis, a suspension in isopropanol was prepared by stirring the solid sample with ultrasound for 10 min. A few drops of the resulting suspension were deposited on a TEM Cu grid (Lacey Carbon Film 300 mesh, Electron Microscopy Science) and subsequently dried and evacuated before the analysis. To estimate the average particle size (d_{TEM}), the particles were considered spherical and the diameter volume–area was calculated by using the following expression: $d_{TEM} = \sum n_i d_i^3 / \sum n_i d_i^2$, where n_i is the number of particles with diameter d_i.

Adsorption measurements of H_2 were carried out in a dynamic equipment with a TCD detector. Samples were reduced in hydrogen at 700 °C for 1 h, then they were cooled in hydrogen up to 400 °C, and subsequently they were treated in Ar flow for 2 h at 400 °C. Finally, the sample was cooled up to room temperature in Ar and pulses of H_2 (0.1 cm^3) were injected in the Ar flow up to reaching saturation. Starting from the consumed H_2 amount, the dispersion was estimated assuming an adsorption stoichiometry H/M^s (M = Ni, Pt).

Temperature programmed reduction experiments (TPR) were carried out in a conventional equipment (Quantachrome Corporation, Qantasorb QS JR-2), with samples of 0.02 g heated from room temperature up to 1000 °C with a heating rate of 10 °C min^{-1} by using a mixture of 5% (v/v) H_2/Ar and a flow of 22 cm^3 min^{-1}.

Diffuse reflectance infrared Fourier transform (DRIFT) spectra were measured in conventional equipment (Fourier

Transform Nicolet Nexus 470) supplied with a diffuse reflectance attachment and with a MCT detector (4000–650 cm^{-1}). Each spectrum was measured with a resolution of 4 cm^{-1}, cumulating 64 scans and was referenced to the spectrum of the catalyst after hydrogen treatment. Before adsorption, samples prereduced ex situ, were heated at 500 °C for 2 h in hydrogen flow, for Pt and Ni catalysts, respectively. After the reduction treatment, the measurement chamber was emptied with He and cooled up to room temperature in He flow. The infrared spectroscopic studies of carbon monoxide adsorption were carried out after the reduction treatment. For that purpose, a CO current diluted in He (10%) was used. Prior to the spectra record, the measurement chamber was emptied with He.

The experimental equipment used for the catalytic tests was a reaction equipment of continuous flow equipped with mass flow meters (Porter Instruments) in each gaseous current (He, CH_4, CO_2 and H_2), electric furnace with temperature controller, quartz reactor of 0.8 mm of internal bore. The gas analysis was carried out by using a chromatograph connected to the experimental unit, CHROMPACK CP9001 model equipped with a column Hayesep D, driven by linear programming of temperature from 25 up to 200 °C. The activity and selectivity of catalysts were determined at atmospheric pressure, feed flow of 200 $cm^3\ min^{-1}$ ($He/CH_4/CO_2$ = 18:1:1), reaction temperatures in the range from 400 to 900 °C. The samples were previously reduced in situ from room temperature up to 700 °C (10° min^{-1}) for 1 h in pure H_2 flow (30 $cm^3\ min^{-1}$).

Stability tests were determined at atmospheric pressure, feed flow of 130 $cm^3\ min^{-1}$. The carbon deposits produced during stability tests were characterized by temperature programmed oxidation (TPO), measuring the weight variation in relation to temperature in a thermo-gravimetric equipment (Shimadzu TGA50). Post-reaction samples of 0.015 g were used feeding with air at flow of 10 $cm^3\ min^{-1}$ and a heating program of 10 °C min^{-1} from room temperature up to 850 °C.

UV–DRS analyses were carried out in a spectrophotometer GBC Cintra 40/UV–vis, equipped with a diffuse reflectance accessory with an integrating sphere. Spectra were recorded in the wavelength range of 300–800 nm. The fresh catalysts and the supports used as targets were analyzed, using α-Al_2O_3 as reference.

3. Results and discussion

Texture and structural properties of α-Al_2O_3 are not affected by the addition of zirconia. BET surface area values are 10 $m^2\ g^{-1}$ for α-Al_2O_3 (A) and α-Al_2O_3-ZrO_2 (AZ) and 60 $m^2\ g^{-1}$ for ZrO_2 (Z). The crystalline structure of pure zirconia, studied by XRD, shows the presence of two crystalline phases, 90% monoclinic and 10% cubic.

Table 1 summarizes the characteristics of the systems studied in this work. Results of metallic particle size (d_{TEM} (nm)) obtained by TEM clearly show a larger particle size for Ni catalysts than for those based on Pt, which is in agreement with the results published [14,28]. These TEM results can be used to estimate values of metallic dispersion; calculated as $D\%$ (TEM) = $97/d_{TEM}$ (nm) for Ni and $D\%$ (TEM) = $108/d_{TEM}$ (nm) for Pt [29]. Table 1 shows that metallic dispersions around 5–7% are obtained for NiAZ and NiA catalysts and 20% for NiZ. Pt catalysts present dispersions around 26–28% for PtAZ and PtA, and a higher value for catalyst supported on ZrO_2 (44%). In principle, this fact would be indicating a higher interaction between the metallic precursor present in the impregnation solution and the ZrO_2 support, compared with supports based on α-Al_2O_3. Dispersion values determined by hydrogen chemisorption (Table 1, $D'\%$ H_2 chemisorption) are compatible with those determined by TEM.

The peak temperatures observed in TPR experiments and the consumption of H_2 values are also shown in Table 1. The reduction profiles are presented in Figs. 1 and 2. For the Ni catalysts (Fig. 1), the temperature peaks of NiA and NiAZ are in the range between 500 and 700 °C. For NiA sample, the most important H_2 consumption peak is observed around 550 °C with a shoulder at around 585 °C, which could be assigned to the presence of NiO_x species in interaction with the support [30–32]. A smaller peak appears at 680 °C that could be assigned to NiO_x species in strong interaction with the support forming, probably, mixed oxide species precursors of $NiAl_2O_4$ [33,34]. The TPR profile for NiAZ sample is very similar with respect to the NiA sample, noticing a shift in all peaks of about 20 °C toward the zone of lowest temperatures, which would indicate a slight modification in the interaction between Ni and the support. Taking into account hydrogen consumptions for NiA and NiAZ, the calculated values correspond to an almost complete reduction ($NiO + H_2 \rightarrow Ni(0) + H_2O$; for 2% in Ni = 341 μmol g^{-1}). From these results, it is possible to

Table 1
Characterization of the studied catalysts

Catalysts	D (%) (TEM)	D' (%) (H_2 chemisorption)	d_{TEM} (nm)	TPR		
				Peaks (°C)		H_2 consumption (μmol g^{-1})
NiA	5.4	2.3	18	552	584–680	320
NiAZ	6.9	4.6	14	530	555–628	300
NiZ	19.4	n.d.	5	445	–	192
PtA	27.0	31.0	4	104	427	95
PtAZ	27.0	n.d.	4	107	423	93
PtZ	43.2	44.0	2.5	220	420	86
Z	–		–	–	620	

Ni dispersions calculated by TEM and H_2 chemisorption ($D\%$, $D'\%$), mean particle size (d_{TEM}) and temperature programmed reduction (TPR).

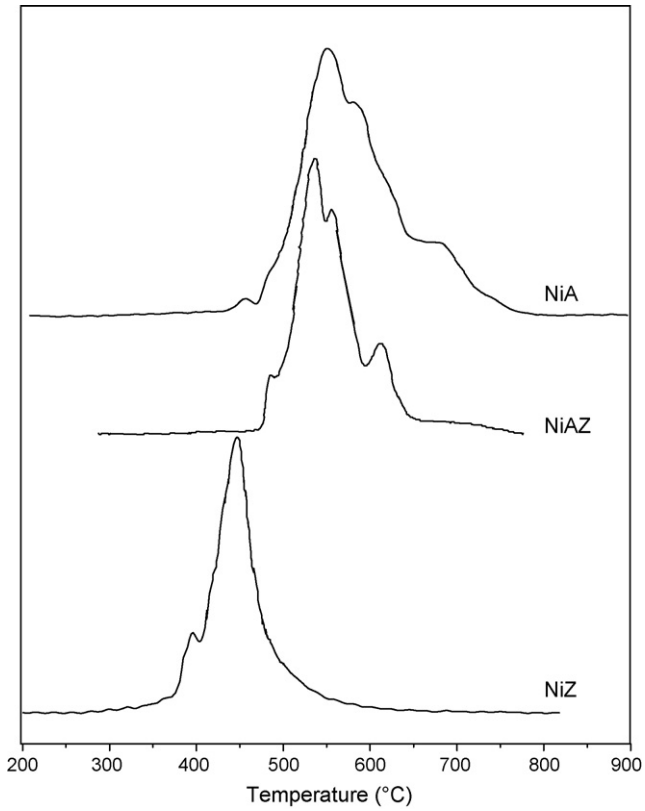

Fig. 1. Temperature programmed reduction (TPR) profiles for Ni catalysts. For the condition, see the text.

assume that the NiO reduction is almost complete for NiA and NiAZ, with absence of free NiO species, so that most part is found as NiO_x species in interaction with the support and/or forming phases of the type mixed oxides precursors of spinels. The support modification with ZrO_2 decreases the temperatures of the reduction peaks, without any other decrease so as to imply a modification in the contribution of the different oxidized species of supported Ni. According to hydrogen consumptions determined for NiAZ, it is not possible to conclude that the ZrO_2 suffers an appreciable reduction process.

The NiZ catalyst displays a shift towards lower temperatures (445 °C) compared to α-Al_2O_3 and α-Al_2O_3-ZrO_2, and this indicates that the metal support interaction is modified, suggesting species of lower specific interaction with ZrO_2 [35]. Taking into account hydrogen consumption for NiZ with respect to NiA and NiAZ, it can be observed that this consumption is sharply reduced, denoting the presence of non-reduced Ni(II) species. According to these results, the reduction of the calcined NiZ sample leads to Ni(0) particles coming from the free NiO species probably separated by ''patches'' of non-reducible Ni(II) interacting with ZrO_x species.

TPR profiles of PtA and PtAZ samples are very similar; they show well differentiated zones of hydrogen consumption. The first zone at relatively low temperatures, between 100 and 250 °C, shows a predominant peak at around 105 °C and a smaller one above 150 °C, which according to literature data would be assigned to platinum oxide and oxychloroplatinum

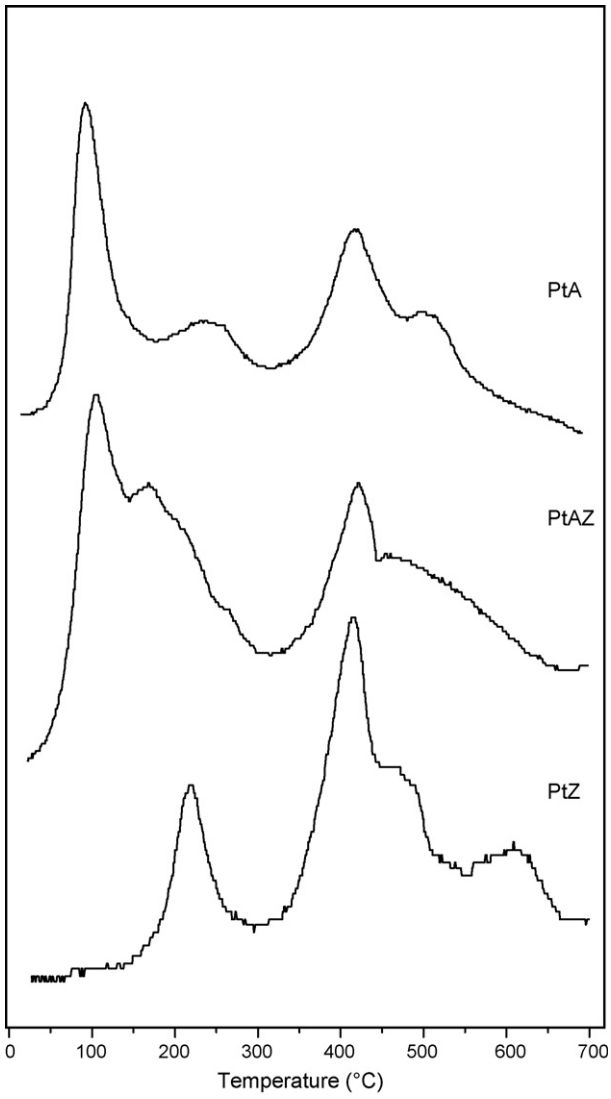

Fig. 2. Temperature programmed reduction (TPR) profiles for Pt catalysts. For the condition, see the text.

surface complex (PtO_xCl_y) [36]. The second zone, at temperatures higher than 400 °C, shows a peak temperature at around 420 °C that could be attributed to a reduction of dispersed platinum in isolated patches onto the support [37]. In both samples the calculated hydrogen consumption corresponds to an almost complete reduction of Pt(IV) ($PtO_2 + 2H_2 \rightarrow Pt(0) + H_2O$; for 1% in Pt = 102 μmol g^{-1}).

The PtZ catalyst displays reduction peaks in three different zones: close to 220 °C, which can also be assigned to the reduction of platinum oxide and oxychloroplatinum surface complex; between 250 and 450 °C, which corresponds to the presence of dispersed platinum oxidized species and finally a small peak at around 620 °C. Taking into account that for ZrO_2, the reduction starts at around 690 °C ((Zr(IV) → Zr(III)) [27], the peak at 620 °C for PtZ sample could be assigned to a slight support reduction. This phenomenon is attributed to the promoted support reduction in platinum presence through hydrogen spillover of hydrogen species [38], which are able to reduce mobile oxygen present in the crystalline structure of the

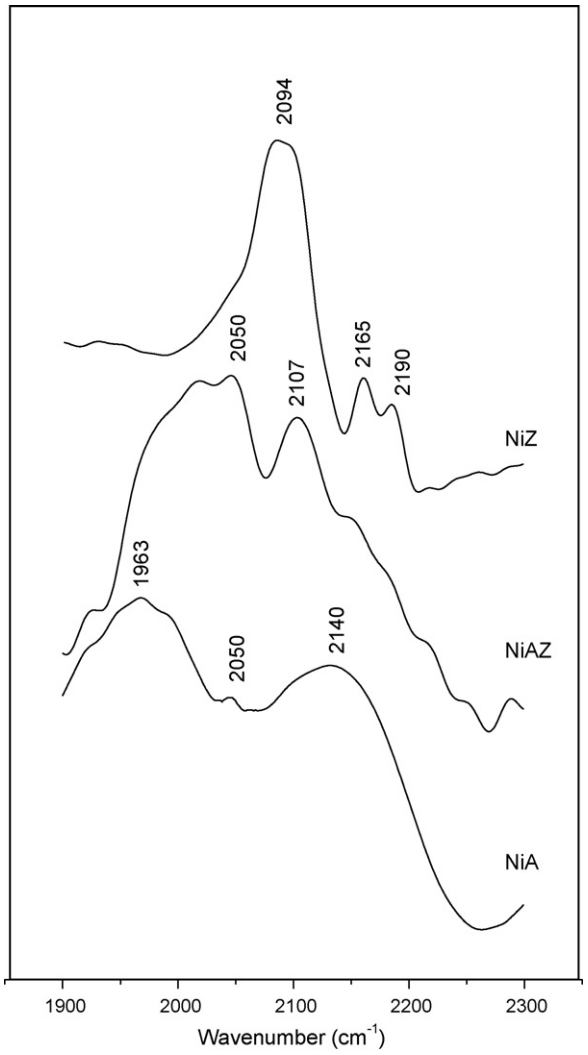

Fig. 3. DRIFT spectra of CO irreversibly adsorbed at room temperature on different Ni catalysts.

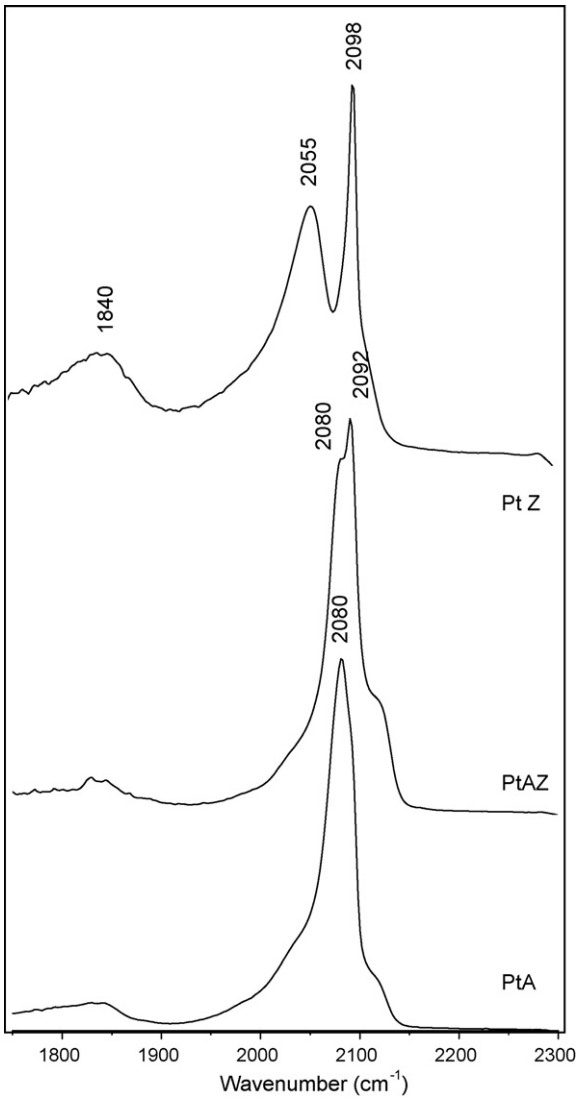

Fig. 4. DRIFT spectra of CO irreversibly adsorbed at room temperature on different Pt catalysts.

support. This fact was not observed for the NiZ sample; although there are no concrete evidences that allow to explain these differences, the highest Pt dispersion (lower particle size) with regard to Ni might be responsible for the aforementioned phenomenon.

DRIFTS results of CO adsorbed on Ni catalysts reduced at 700 °C are shown in Fig. 3. Usually there are two types of CO adsorbed on Ni sites in the region 2100–1900 cm^{-1}: linear CO adsorption between 2100 and 2000 cm^{-1} and bridged CO adsorption below 2000 cm^{-1} [39–42].

Respect to the bands between 2100 and 2000 cm^{-1}, differences are observed between Ni catalysts, which could be assigned to differences in the metallic dispersion. The bands above 2100 cm^{-1} are present in all samples and may be attributed to CO adsorption on the small Ni fraction not reduced in catalysts NiA or NiAZ. The NiZ sample displays bands above 2100 cm^{-1} that can also be assigned to ionic Ni or to a Zr(IV)–CO interaction as it is observed by Souza et al. for Pt/ZrO_2 [27]. In catalysts NiA and NiAZ, bands at about 1960 cm^{-1} can be observed assigned to CO bridged adsorption, characteristic of Ni species less dispersed on the surface [40].

DRIFTS results for Pt catalysts are shown in Fig. 4. According to Saussey and co-workers [43], the linear CO–Pt_{red} band is around 2050 cm^{-1} for isolated vibration and increases with surface coverage due to the vibrational coupling. Thus, there may be two linear species of adsorbed CO on reduced platinum; one in the region close to 2090 cm^{-1}, corresponding to a dense atom group (type I, Pt(1 1 1)) and the other close to 2080 cm^{-1} region, corresponding to less dense atom group (type II, Pt(1 0 0)), respectively [44,45].

PtA and PtAZ samples (Fig. 4) display bands at 2080 and 2090 cm^{-1} presenting different contributions of CO type I and CO type II species, depending on the support. The contribution of linear adsorbed CO species of type I on PtAZ is higher than on PtA, whereas linear species of type II prevail on PtA. Two bands are observed in the PtZ sample; one at 2050 cm^{-1} assigned to isolated sites of reduced Pt and the other one in the region of 2090 cm^{-1} attributed to a dense atom group (type I, Pt (1 1 1)). The signal close to 1840 cm^{-1} is present in all Pt samples corresponding to bridged type species of CO adsorbed

on reduced Pt [46]. In the region above 2100 cm^{-1}, one peak has been observed, mainly for PtAZ, which can either be assigned to CO adsorbed on platinum oxide (Pt(II)) or to CO on Zr(IV) of the support (around 2120 cm^{-1}) [27,47].

The diffuse reflectance spectroscopy (DRS) provides important complementary information to the characterization, mainly in the case of Ni samples. As it is shown by TPR diagrams for NiA and NiAZ, the reduction temperatures above those of NiO bulk suggest NiO_x species in strong interaction with the support forming probably mixed oxide species precursors of $NiAl_2O_4$. This fact leads to the development of spinels or mixed oxides precursors of spinels. Generally, these Ni spinels are partially inverted, and it means that not all Ni cations are in tetrahedral coordination and not all Al cations are in octahedral coordination. The inversion degree can be represented by the fraction of Al cations in tetrahedral coordination [33,48]. DRS results allow estimating the relationship between Ni(II) ions in tetrahedral and octahedral coordination present in each Ni catalyst. The literature reports that Ni(II) ions in octahedral symmetry (Oh) present bands at 350, 440, 460 and 720 nm; while Ni(II) ions in tetrahedral symmetry (Td) present the three characteristic bands at 550, 600 and 640 nm, and a less pronounced band at 720 nm [49,50].

DRS spectra are shown in Fig. 5. As it has been mentioned, the inversion degree of Ni spinels leads to a greater contribution of Ni(II)Oh. Comparing NiAZ with NiA, the latter presents a smaller signal of Ni(II)Td, and this would indicate the presence of a superficial spinel precursor with an inversion degree greater in NiAZ than in NiA. On the other hand, for the NiZ catalyst the spectrum of Fig. 5 only shows bands corresponding to Ni(II) in Oh, indicating NiO in agreement with TPR diagram for NiZ, which shows a temperature peak around 400 °C, corresponding to a bulk NiO.

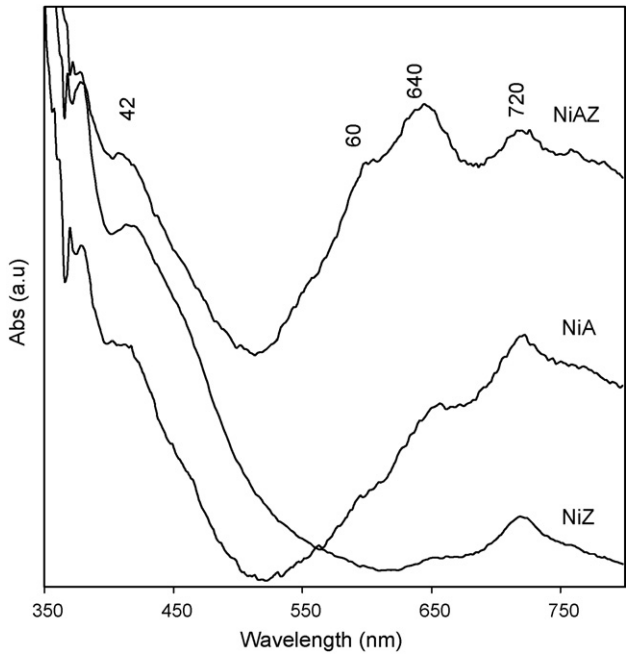

Fig. 5. Diffuse reflectance UV–vis absorption spectra of oxidized Ni catalysts.

Concerning the catalytic activity in the dry reforming reaction (DR), results of catalytic tests as function of the reaction temperature are shown in Fig. 6a and b. In order to compare initial specific activities, TOF values (Table 2) were estimated at 550 °C (s^{-1}, expressed as CH_4 molecules reacted per second per superficial metallic atom). According to these results: (i) Ni is slightly more active than Pt and (ii) both, Ni and Pt, present good activity levels; TOF between 1.7 and 3.7 s^{-1} for Ni samples and between 1 and 1.7 s^{-1} for Pt samples.

With respect to the selectivity, expressed as a molar ratio H_2/CO, for all catalysts it is maintained in values between 0.9 and 1 (at 650 °C) near to the corresponding stoichiometric relationship for DR reaction.

Stability is as important as activity on the catalytic behavior. For this process, the catalysts may undergo two main deactivation mechanisms: sintering of the active phase and carbon deposition. The latter may result from the already mentioned CO disproportionation (''Boudouard reaction''), thermodynamically favored at low temperatures, or from CH_4 decomposition, thermodynamically favored at high temperatures. In this work, the stability is studied for DR reaction at 700 °C for 50 h, where CH_4 decomposition is thermodynamically favored. Fig. 7 shows the evolution of activity coefficient a_{CH_4} in relation to the reaction time; a_{CH_4} represents the relationship between the consumption rate of CH_4 with time on stream and the initial consumption rate. It is observed that the NiZ, PtA and NiA present low stability levels, with activity coefficients (a_{CH_4}) below 0.2.

The average particle size and carbon content in the post-reaction samples (50 h; Table 2) were determined by TEM and TPO/TGA, respectively. Table 2 reports also the variation of mean particle size of post-reaction catalyst with respect to the fresh catalyst. From these results, it is reasonable to conclude that under our operating conditions, there is a strong sintering contribution to deactivation in NiZ catalyst (d_{TEM} incresase = 260%), whereas for the other catalysts a small growth of particle size during reaction is observed (approximately 50%).

With respect to carbon formation, results observed in Table 2 show that, for Ni as well as for Pt, the systems supported on α-Al_2O_3 non-modified by ZrO_2 present the highest levels of deposited carbon; while when comparing both metals, systems based on Ni lead to higher carbon concentrations on post-reaction samples than systems based on Pt. As example, the carbon amount deposited determined by TPO/TGA was 7 wt% for NiA and 0.6 wt% for PtA. Fig. 7 shows that the PtA catalysts presents a higher initial deactivation rate than the one of NiA, which is in agreement with that reported by Nagaoka et al. [22,23] who observed a strong Pt poisoning when the first carbon atoms begin to be deposited. After 70 reaction hours, a_{CH_4} values are similar for PtA and NiA (between 0.1 and 0.2), in spite of the marked differences observed in the total carbon amount deposited. This fact can be explained by the carbon nature formed as function of the metal, as it could be verified by TEM micrographs. For Ni catalysts the metal can dissolve unreactive C residues and generate carbon filaments (whiskers) with the Ni particle on the filament top, thus resulting in much

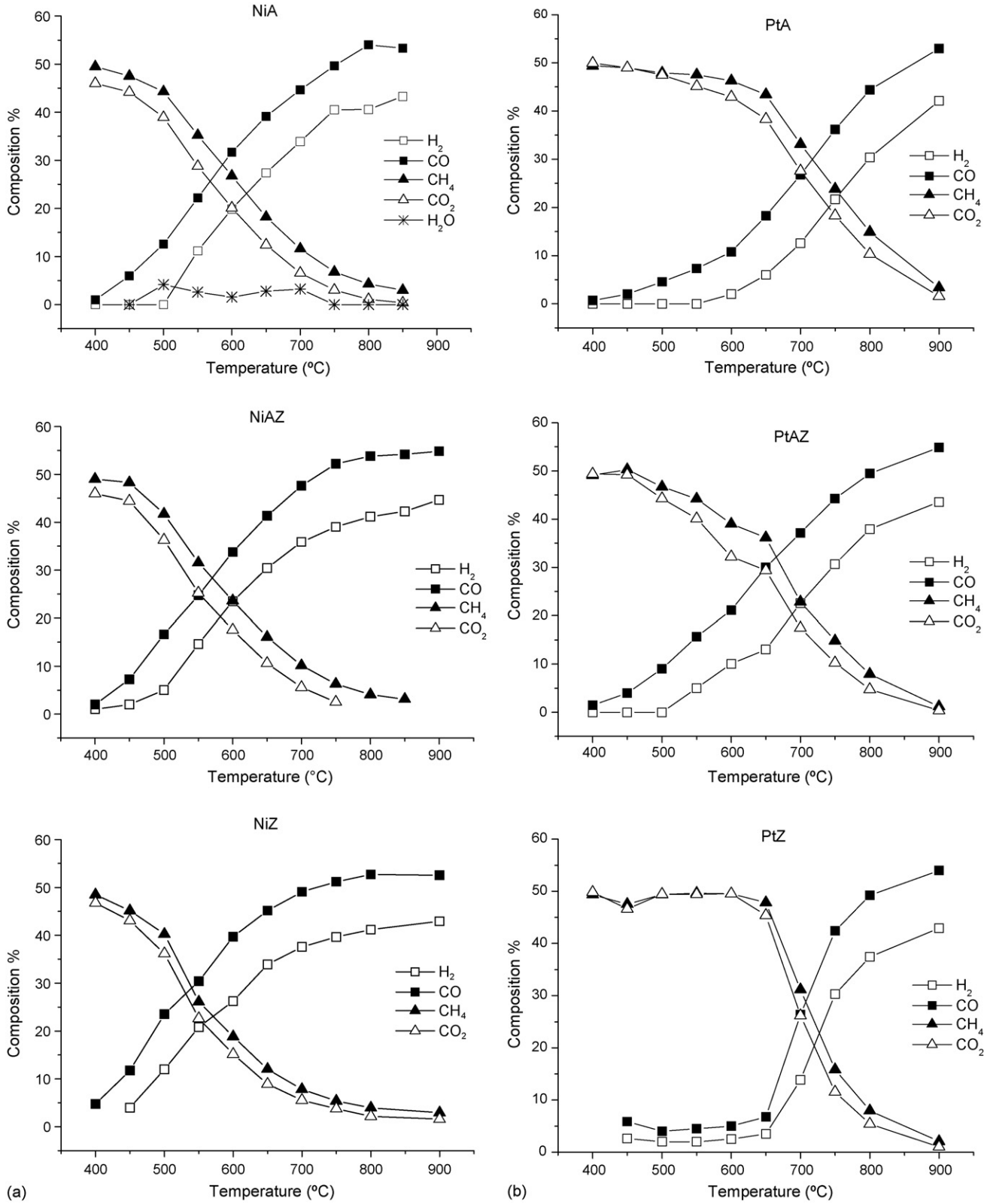

Fig. 6. (a) Methane conversion of Ni catalysts for CO_2 reforming as a function of temperature (each point was taken after 30 min on stream) and (b) methane conversion of Pt catalysts for CO_2 reforming as a function of temperature (each point was taken after 30 min on stream).

lower deactivation rates than those expected if metal-covering coke deposits occurred. Pt is not able to dissolve unreactive carbon and so, in Pt catalysts, metallic particles are gradually covered by coke leading to catalyst deactivation.

It is evident that the ZrO_2 presence plays a fundamental role in minimizing the carbon formation process. In the NiAZ system, DRIFTS results allow us to conclude that Ni is deposited in close contact with the ZrO_2 that modifies the

Table 2
Initial TOF values at 550 °C (s^{-1}), activity coefficient after 50 h (a_{CH_4}), particle size and carbon content in the post-reaction samples

Catalyst	TOF (s^{-1})	a_{CH_4} after 50 h	d_{TEM} (nm) fresh	d_{TEM} (nm) post-reaction	d_{TEM} increase (%)	C (p/p%)
NiA	3.7	0.20	18	25	39	7
NiAZ	3.0	0.50	14	19	36	0.9
NiZ	1.7	0	5	18	260	0.6
PtA	1.7	0.10	4	6	50	0.6
PtAZ	1.7	0.40	4	6	50	<0.1
PtZ	1	0.75	2.5	4	60	<0.1

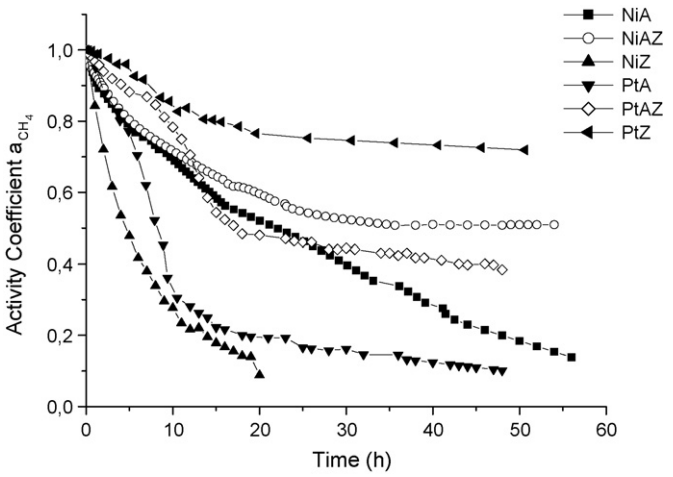

Fig. 7. Deactivation tests of the studied catalysts at 700 °C. For the conditions, see the text.

α-Al_2O_3 support. According to the literature [8,27], it can be suggested that CO_2 adsorbs dissociatively (stage a) on the boundary between ZrO_2 and Ni, favoring the gasification of unsaturated intermediates (stage b) and precursors of carbon deposits and thus avoiding the formation of characteristic filaments in these systems (stage c).

$$CO_2{-}S + 2S \rightarrow CO{-}S + O{-}S \quad (a)$$

$$CH_x{-}S + O{-}S + (x-1)S \rightarrow CO{-}S + xH{-}S \quad (b)$$

$$CH{-}S + S \rightarrow C{-}S + H{-}S \quad (c)$$

4. Conclusions

Catalysts based on nickel and platinum supported on α-Al_2O_3, α-$Al_2O_3 + ZrO_2$ and ZrO_2 were prepared by impregnation. In all cases, better values of metallic dispersion were obtained in Pt catalysts with respect to Ni catalysts; for example, 7% for NiAZ and 27% for PtAZ.

Concerning the catalytic behavior in the syngas obtention via dry reforming reaction: (i) Ni is slightly more active than Pt and (ii) both, Ni and Pt, present good activity levels; TOF between 1.7 and 3.7 s^{-1} for Ni samples and between 1 and 1.7 s^{-1} for Pt samples. The selectivity measured at 650 °C, expressed by the molar ratio H_2/CO, reached values near to 1.

With respect to the stability, PtZ, PtAZ and NiAZ systems present clearly a better performance than the ones supported on alumina not modified by ZrO_2. PtZ, PtAZ and NiAZ show lower deactivation level as function of reaction time, reaching a plateau in the conversion after first 15 reaction hours. This higher stability is related with a strong decrease in the carbon amount deposited, which is explained by the ZrO_2 presence that plays a fundamental role in minimizing the carbon formation process, promoting the dissociation chemisorption of CO_2 that enables the gasification of carbon intermediate precursors responsible for the deactivation mechanism in DR.

Acknowledgements

This work was financed by ANPCyT (PICT 14122), CONICET (PIP 6527) and International Project of Collaboration between CONICET (Argentina) and CNPq (Brazil).

References

[1] J.R. Rostrup-Nielsen, L.J. Christiansen, Appl. Catal. A 126 (1995) 381.
[2] E. Ruckenstein, Y. Hang Hu, Appl. Catal. A 133 (1995) 149.
[3] J.M. Wei, B.Q. Xu, J.L. Li, Z.X. Cheng, Q.M. Zhu, Appl. Catal. A 196 (2000) L167.
[4] S. Wang, G.Q. Lu, Appl. Catal. B 19 (1998) 267.
[5] T. Osaki, T. Mori, J. Catal. 204 (2001) 89.
[6] J. Wei, E. Iglesia, J. Catal. 224 (2004) 370.
[7] N.N. Nichio, M. Casella, O.A. Ferretti, M. González, C. Nicot, B. Moraweck, R. Frety, Catal. Lett. 42 (1996) 65.
[8] F. Pompeo, N.N. Nichio, O.A. Ferretti, D.E. Resasco, Int. J. Hydrogen Energy 30 (2005) 1399.
[9] O.W. Perez Lopez, A. Senger, N.R. Marcilio, M.A. Lansarin, Appl. Catal. A 303 (2006) 234.
[10] Z. Hou, O. Yokota, T. Tanaka, T. Yashima, Appl. Catal. A 253 (2003) 381.
[11] H.Y. Wang, E. Ruckenstein, Appl. Catal. A 209 (2001) 207.
[12] Y. Chen, J. Ren, Catal. Lett. 29 (1994) 39.
[13] B.S. Liu, C.T. Au, Appl. Catal. A 244 (2003) 181.
[14] N.N. Nichio, M.L. Casella, G.F. Santori, E.N. Ponzi, O.A. Ferretti, Catal. Today 62 (2000) 231.
[15] F. Arena, F. Frusteri, A. Parmaliana, Appl. Catal. A 187 (1999) 127.
[16] J.S. Chang, S.E. Park, J.W. Yoo, J.N. Park, J. Catal. 195 (2000) 1.
[17] F. Pompeo, N.N. Nichio, M.G. González, M. Montes, Catal. Today 107–108 (2005) 856.
[18] A.T. Ashcroft, A.K. Cheetham, M.L.H. Green, P.D.F. Vernon, Nature 225 (1991) 352.
[19] J.R. Rostrup Nielsen, J. Catal. 144 (1993) 38.
[20] J. Múnera, S. Irusta, L. Cornaglia, E. Lombardo, Appl. Catal. A 245 (2003) 383.
[21] S. Irusta, L.M. Cornaglia, E.A. Lombardo, J. Catal. 210 (2002) 263.
[22] K. Nagaoka, K. Seshan, K. Aika, J. Lercher, J. Catal. 197 (2001) 34.
[23] K. Nagaoka, K. Seshan, J. Lercher, K. Aika, Catal. Lett. 70 (2000) 109.
[24] C. Jung, R. Ishimoto, H. Tsuboi, M. Koyama, A. Endou, M. Kubo, C. Del Carpio, A. Miyamoto, Appl. Catal. A 305 (2006) 102.
[25] T.G. Kuznetsova, V.A. Sadykov, S.A. Veniaminov, G.M. Alikina, E.M. Moroz, V.A. Rogov, O.N. Martyanov, V.F. Yudanov, I.S. Abornev, S. Neophytides, Catal. Today 91–92 (2004) 161.

[26] F. Dong, A. Suda, T. Tanabe, Y. Nagai, H. Sobukawa, H. Shinjoh, M. Sugiura, C. Descorme, D. Duprez, Catal. Today 90 (2004) 223.
[27] M.M.V.M. Souza, D.A.G. Aranda, M. Schmal, J. Catal. 204 (2001) 498.
[28] G.F. Santori, M.L. Casella, G.J. Siri, H.R. Adúriz, O.A. Ferretti, React. Kinet. Catal. Lett. 75 (2) (2002) 225.
[29] R.J. Farrauto, C.H. Bartholomew, Fundamentals of Industrial Catalytic Processes, Blackie Academic & Professional. Chapman & Hall, 1997„ p. 81.
[30] H.-S. Roh, K.-W Jun, S.-C. Baek, S.-E. Park, Catal. Lett. 81 (2002) 147.
[31] H.-S. Roh, K.-W. Jun, S.-E. Park, Appl. Catal. A 251 (2003) 275.
[32] H.-S. Roh, K.-W. Jun, W.-S. Dong, S.E. Park, Y. -Joe, Chem. Lett. 30 (7) (2001) 666.
[33] R. Molina, G. Poncelet, J. Catal. 173 (1998) 257.
[34] J.L. Villacampa, C. Royo, E. Romeo, A. Montoya, P. Del Angel, A. Monzón, Appl. Catal. A 252 (2003) 363.
[35] P. Moulijn, J.A. Arnoldy, J. Catal. 93 (1985) 38.
[36] H. Lieske, G. Lietz, H. Spindler, J. Völter, J. Catal. 81 (1983) 8.
[37] M.J. Tiernan, O.E. Finlayson, Appl. Catal. B 19 (1998) 23.
[38] L.V. Mattos, E.R. de Oliveira, P.D. Resende, F.B. Noronha, F.B. Passos, Catal. Today 77 (2002) 245.
[39] J.B. Peri, J. Catal. 86 (1984) 84.
[40] M. Hair, Infrared Spectroscopy in Surface Chemistry, Marcel Dekker Inc., New York, 1967.
[41] M. Mihaylov, K. Chakarova, K. Hadjiivanov, J. Catal. 228 (2004) 273.
[42] G. Poncelet, M.A. Centeno, R. Molina, Appl. Catal. A 288 (2005) 232.
[43] J.L. Freysz, J. Saussey, J.C. Lavalley, P. Bourges, J. Catal. 197 (2001) 131.
[44] A. Ghorbel, M. Primet, J. Chim. Phys. 73 (1976) 89.
[45] P. Pillonel, S. Derrouiche, A. Bourane, F. Gaillard, P. Vernoux, D. Bianchi, Appl. Catal. A 278 (2005) 223.
[46] X. Mugniery, T. Chafik, M. Primet, D. Bianchi, Catal. Today 52 (1999) 15.
[47] J.J. Daniels, A.R. Arther, B.L. Lee, S.M. Stagg-Williams, Catal. Lett. 103 (3–4) (2005) 169.
[48] M. Lo Jacomo, M. Schiavello, A. Cimino, J. Phys. Chem. 75 (1971) 1044.
[49] B. Scheffer, J.J. Heijeinga, J.A. Moulijn, J. Phys. Chem. 91 (1987) 4752.
[50] K. Hadjiivanov, M. Mihaylov, D. Klissurski, P. Stefanov, N. Abadjieva, E. Vassileva, L. Mintchevz, J. Catal. 185 (1999) 314.